Small-Angle X-ray and Neutron Diffraction from Corneal Stroma

(Extended Abstract only) By G. F. ELLIOTT, J. M. GOODFELLOW and A. E. WOOLGAR, *Open University Research Unit, Boars Hill, Oxford, England* and P. A. TIMMINS, *Institute Laue–Langevin, Grenoble, France*

The corneal stroma is a connective tissue which combines the usual properties of strength and resilience with one property, transparency, unusual in such tissues. Several models have been put forward to account for this transparency, these differ in detail but in almost all cases the regularity of arrangement of the collagen fibrils is taken to be an important parameter of the model (Maurice, 1957; Farrell & Hart, 1969; Benedek, 1971). So far the only experimental evidence about this arrangement comes from electron microscopy, and we have therefore applied small-angle diffraction techniques because they involve less preparative procedures which might cause artifacts.

Excised stroma swells when placed in an excess of aqueous solution, and in swelling it loses its transparency. We have observed a long spacing corresponding to the centre-to-centre distance of the collagen fibrils, and have followed this spacing as a function of the hydration of the tissue with both X-ray and neutron diffraction. The spacing changes from about 40 nm in nearly dry tissue to as much as 130 nm in very hydrated tissue (hydration, *i.e.* ratio of water to dry weight ~ 19); the square of this interfibrillar spacing is proportional to the hydration. Changes in pH and ionic strength of the bathing solution affect the time course of the swelling, but our results (particularly from neutron diffraction) show that at least to a first approximation, the spacing *at a given hydration* does not depend on these parameters. Contrast matching experiments with neutron diffraction, where the aqueous medium has various H_2O/D_2O ratios, show the interfibrillar reflection to have a minimum (effectively zero) intensity at a water content of about 45% D_2O/H_2O. This is almost identical to the match point for the first-order meridional reflection from rat-tail collagen (Miller *et al.*, 1976). As this latter reflection arises primarily from the protein-gap step function the contrast behaviour of the interfibrillar reflection shows that the fibril-interspace system behaves as if the interfibrillar space were simply an expandable aqueous medium between protein (collagen) fibrils.

We have also observed the third and fifth orders of the

(67 nm) collagen spacing: these do not change with tissue hydration, for example at a tissue hydration of 15 the collagen spacing observed from the third and fifth orders is 67.3 nm, while the interfibrillar spacing is about 110 nm. The absence of the first-order collagen spacing is surprising: we think it may be due to the occlusion of the gap between corneal collagen molecules, perhaps by the glycoproteins and glycosaminoglycans in this tissue. Calculations on the neutron scattering-length densities for collagen and for glycosaminoglycans show them to be very similar and to have similar contrast-variation behaviour in different H_2O/D_2O mixtures. This would be consistent with our inability to observe the first-order meridional reflection by matching out the glycosaminoglycan contribution. (The errors in this calculation are however quite large because of the uncertainty of the specific volume of the glycosaminoglycans within the tissue.) Certainly corneal collagen fibrils are unusual in their uniform size and in their band pattern observed in the electron microscope.

In contrast the collagen fibrils of the sclera (the major non-transparent part of the eyeball), which are non-uniform in diameter, do show a first-order collagen reflection. Further details of the X-ray part of this study can be found in Goodfellow, Elliott and Woolgar (1978).

References

BENEDEK, G. B. (1971). *Appl. Opt.* **10**, 459–473.
FARRELL, R. A. & HART, R. W. (1969). *Bull. Math. Biophys.* **31**, 727–759.
GOODFELLOW, J. M., ELLIOTT, G. F. & WOOLGAR, A. E. (1978). *J. Mol. Biol.* **119**, 237–252.
MAURICE, D. M. (1957). *J. Physiol. (London).* **136**, 263–286.
MILLER, A, BRODSKY DOYLE, B., HULMES, D. J. S., JENKIN, G. T., WHITE, J. W., HAAS, J., IBEL, K. & TIMMINS, P. A. (1976). *Neutron Scattering for the Analysis of Biological Structures. Brookhaven Symp. Biol.* **27**, III: 86–100.

Small-Angle X-ray Studies of the Scaffold in Bacteriophage λ Head Formation

(Extended Abstract only) By PETER KÜNZLER and HANS BERGER, *Biozentrum der Universität Basel, Department of Structure Biology, Klingelbergstrasse 70, 4056 Basel, Switzerland*

The pathway of bacteriophage λ head formation has been well characterized *in vivo* and *in vitro* (Hohn, Katsura & Hohn, 1977). First a petit λ particle consisting of a shell

protein pE, a protein pNu3 and minor proteins, but lacking DNA, is formed. The pNu3-containing structure is then converted to a structure which does not contain pNu3, and

which is capable of taking up and cutting the viral DNA. The purpose of this work is to determine the scaffold structure, formed by pNu3, by small-angle scattering techniques based on the known physico-chemical properties of pNu3-containing and pNu3-lacking particles (Künzler & Hohn, 1978). The scaffold is found to be inside the protein shell but less concentrated than the 130 Å radius core reported from electron micrographs.

Because phage strains defective in gene Nu3 produce abortive head intermediates, pNu3 is thought to be involved in the *construction* of the proper *head* precursor. Since some of these abortive structures contain shell protein pE monomers arranged in a two-dimensional hexagonal lattice
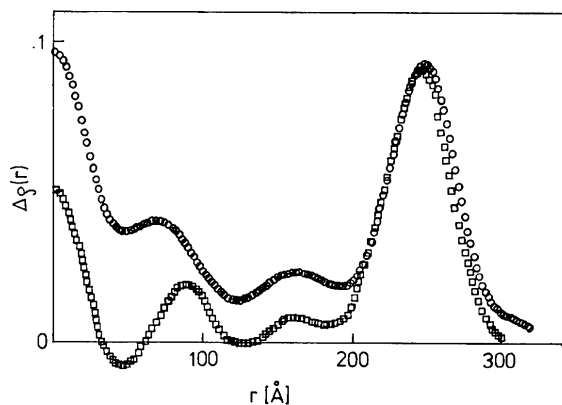

Fig. 1. Radial density distribution of pNu3-containing (O) and pNu3-lacking (□) particles. $\Delta\varrho$ in e Å^{-3}. Ten diffraction orders were Fourier transformed, corresponding to a maximal s value of about (50 Å)$^{-1}$. Temperature factor 0·1 [$s = (1/\lambda) \sin(\theta/2)$].
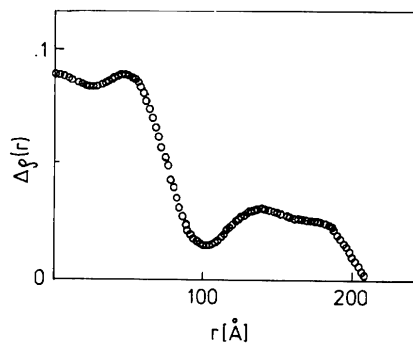

Fig. 2. Difference density distribution obtained by taking the Fourier transform of the difference of the amplitudes of pNu3-contaning and pNu3-lacking particles. Data were scaled together by extrapolating intensities to zero angle and taking a molecular-weight ratio of 22:18. $\Delta\varrho$ in e Å^{-3}. Temperature factor 0·1. A very similar density distribution was obtained by taking directly the difference between the two density distributions shown in Fig. 1.

(Wurtz, Kistler & Hohn, 1976), the main role of the structure formed by pNu3 probably is to serve as a *template* or *scaffold* for the formation of a closed icosahedral shell formed by pE, which otherwise would arrange itself hexagonally.

The material was prepared and controlled for purity and monodispersivity as described in Künzler & Hohn (1978). Small-angle X-ray scattering was performed at a wavelength of 1·54 Å with a Kratky camera (solutions) and a Franks point-focusing camera (pellets). Deconvolution of the diffraction patterns produced by the Kratky camera was done iteratively (Glatter, 1974). The films obtained from the Franks camera were scanned with an Optronics scanner, 25 μm steps being used, and the data circularly integrated. Measurements in solution were performed at four different concentrations in the range of about 50 mg/ml to 4 mg/ml for both species of particles.

Up to the present we have been able to measure ten diffraction maxima. No concentration dependence of the results from the solution scattering was observed. The third- and higher-order maxima measured by the point-focusing camera on pellets coincide with maxima from solution scattering after deconvolution (results not shown). Amplitudes were calculated from intensities with alternating signs assumed. Radial electron density distributions obtained from Fourier transformation of these amplitudes for particles both containing pNu3 and lacking pNu3 are shown in Fig. 1. In Fig. 2 we have plotted the Fourier transform of the difference between the amplitudes of pNu3-containing and pNu3-lacking particles scaled together by using molecular weights determined from sedimentation and diffusion coefficients (see legend to Fig. 2).

From Figs. 1 and 2 we find that the scaffold must be located inside the protein shell, the electron density distribution being consistent with the molecular-weight ratio of scaffold to shell of about 20%, as measured by other methods (Künzler & Hohn, 1978). Our results are, however, incompatible with the location of most of the scaffold mass in a central 'core' of about 130 Å radius obtained from electron micrographs of thin sections (Zachary, Simon & Litwin, 1976).

This study will be submitted to the *Journal of Molecular Biology*.

References

GLATTER, O. (1974). *J. Appl. Cryst.* **7**, 147–153.
HOHN, T., KATSURA, I. & HOHN, B. (1977). *Curr. Top. Microbiol. Immunol.* **78**, 69–110.
KÜNZLER, P. & HOHN, T. (1978). *J. Mol. Biol.* In the press.
WURTZ, M., KISTLER, J. & HOHN, T. (1976). *J. Mol. Biol.* **101**, 39–56.
ZACHARY, A., SIMON, L. D. & LITWIN, S. (1976). *Virology*, **72**, 429–442.